Journal of ELECTRONIC MATERIALS, Vol. 49, No. 1, 2020
https://doi.org/10.1007/s11664-019-07742-1


TMS2019 MICROELECTRONIC PACKAGING, INTERCONNECT, AND PB-FREE SOLDER

# Tuning Stress in Cu Thin Films by Developing Highly (111)-Oriented Nanotwinned Structure

I-JU WANG,[1] CHING-SHUN KU,[2] TU-NGOC LAM,[1] E-WEN HUANG,[1] K.N. TU,[3] and CHIH CHEN[1,4]

1.—Department of Materials Science and Engineering, National Chiao Tung University, 1001 University Road, Hsinchu 30010, Taiwan, ROC. 2.—National Synchrotron Radiation Research Center, Hsinchu 30076, Taiwan, ROC. 3.—Department of Materials Science and Engineering, University of California at Los Angeles, Los Angeles, CA, USA. 4.—e-mail: chih@mail.nctu.edu.tw

We have examined the effect of different bath temperatures on residual stress of both the random-oriented Cu films and the highly (111)-oriented nanotwinned Cu films by synchrotron radiation x-ray measurements. The bath temperature varied from 15°C to 40°C. The results indicate that the average residual stress in the highly (111)-oriented nanotwinned films is higher than that in the randomly oriented Cu films. However, the stress in the highly (111)-oriented Cu decreases with increasing bath temperature. The average residual stress can be reduced from 253 MPa electroplated at 15°C to 95 MPa under a bath temperature of 35°C. We could successfully tune and measure residual stress of the Cu thin films. The films with low residual stress prevent warpage from occurring on the substrate and lower the processing failure in copper direct bonding and other processes that need alignment.

**Key words:** Residual stress, nanotwinned Cu, electroplating, synchrotron x-ray diffraction

## INTRODUCTION

As Moore's law is reaching a limit in the microelectronic industry, a three-dimensional integrated circuit (3D IC) has been developed as an upgrade from the 2D IC in order to meet new requirements.[1] This is mainly driven by factors such as form factor reduction of the overall package and poor large die yields. The 3D IC requires new packaging technology, such as copper direct bonding and fine-line fan-out technology. Integrated fan-out wafer level package (InFOWLP) technology has made groundbreaking advances and is currently the mainstream package technology for consumer electronic products. Compared with traditional flip chip wafer level packaging (FCWLP) technology, InFOWLP possesses superior advantages such as higher pin count, lower power consumption, higher electrical performance, better heat dissipation, and overall low cost.[2,3] However, in FOWLP, an epoxy molding compound (EMC) is integrated with Si, causing thermal stress to become a reliability issue because of its different thermal expansion coefficients.[4,5] After performing thermal cycling tests, the Cu interconnects in the redistribution layer across the interface between EMC and Si show serious fracture failure.[6] To overcome high stress issues, nanotwinned Cu (nt-Cu) has been proposed and applied as a promising replacement material for interconnects due to its higher mechanical strength than bulk Cu while maintaining the same resistivity.[7–10] Furthermore, nt-Cu increases electromigration resistance of the interconnects[11–14] while also possessing high thermal stability.[15] The characteristic of low oxidation rate could significantly decrease the cleansing time in IC processing.[16]

Chen et al.[17] have discovered that the microstructure and the intensity of (111)-oriented Cu thin films change under different bath temperatures

(Received May 12, 2019; accepted October 17, 2019; published online November 12, 2019)

during electroplating, and in turn the residual stress may be influenced.[18] However, they didn't measure the residual stress in the film. It's reported that residual stress in the materials affects life prediction and structural reliability in the products. Residual stress causes deformation in materials during reliability tests and also lowers the fatigue strength.[19]

In this study, we address the relationship between bath temperatures and thin film residual stress. We fabricate random-oriented Cu and highly (111)-oriented Cu thin films under different bath temperatures for comparison. Our objective is to tune and measure the residual stress of nt-Cu thin films. It's important to evaluate the stress in Cu thin films to help us understand its characteristics.

## EXPERIMENTAL

Si wafers with an adhesion layer of 200-nm-thick TiW and a seed layer of 200-nm-thick Cu were sequentially sputtered on the Si wafer by an Oerlikon ClusterLine 300 and adopted as the substrate. The Cu seed layer with highly (111)-preferred orientation was necessary to aid growth of the nt-Cu microstructure.[20]

The substrate was first rinsed with citric acid to remove surface oxide and then cleaned with acetone to remove organic compounds. After the cleansing process, the substrate was placed at the cathode and a high-purity (99.99%) Cu sheet as the anode for the electroplating process. The electrolyte was a $CuSO_4$ solution with 40 ppm hydrochloride acid and surfactants. The deposition area was $3 \times 3$ cm$^2$ and approximately 3-$\mu$m thick. The Cu thin films were electroplated under four different bath temperatures; 15°C, 25°C, 35°C, and 40°C. The stirring rate was 1200 rpm and the current density was 50 mA cm$^{-2}$ to 120 mA cm$^{-2}$.

The microstructure and thickness of Cu thin films were examined by a dual-beam focused ion beam (DB-FIB, FEI 200). The distribution of grain orientation was measured by electron backscattered diffraction (EBSD, EDAX/TSL technology). High-resolution x-ray (D8 DISCOVER) diffraction was employed to observe the grain orientation.

The $\cos^2\alpha\sin^2\Psi$ residual stress measurement used in past researches[21,22] was performed using beamline 17B, general x-ray scattering/diffraction at the National Synchrotron Radiation Research Center (NSRRC), Taiwan. Each of the samples was tilted in nine different $\Psi$ angles, 0°, ± 23°, ± 33°, ± 43° and ± 53° during the $\Psi$ scan. Each set of $\Psi$ scan was performed with eight various $\Phi$ angles, 0°, 30°, 45°, 90°, 120°, 135°, 150° and 180°. The incident angle was 0.6° and the wavelength of the synchrotron radiation was 0.15498 nm. The Cu (200) peak was chosen for the strain measurement. The $\cos^2\alpha\sin^2\Psi$ residual stress calculation with $\Phi$ angle scan was used to measure the texture of the sample in order to increase its measurement volume.[21] The residual stress of thin films was calculated by Eq. 1:

$$\frac{d_{\Psi}(\Phi) - d_0}{d_0} = \frac{1+v}{E}\sigma\cos^2\alpha\sin^2\Psi + \frac{1+v}{E}\alpha\sin^2\alpha - \frac{2v}{E}\sigma \tag{1}$$

where $d_0$ was the initial lattice spacing at $\Psi = 0$, $d_\Psi$ was the lattice spacing for every tilted $\Psi$ angle. $E$ and $v$ were the Young's modulus and Poisson's ratio of the material, respectively, and $\sigma$ was the residual stress of thin films. Each Bragg peak was applied to the Voigt function by OriginPro fitting function. After the fitting we can get the center 2Θ value in each Bragg peak and then calculate $d$-spacing. As shown in Fig. 1, the residual stress could be derived from the slope in the $(d_\Psi - d_0)/d_0$ versus $\cos^2\alpha\sin^2\Psi$ plot. The effective moduli in random-oriented Cu and highly (111)-oriented Cu were 115.2 GPa and 130.0 GPa, respectively.[23] The effective Poisson's ratio in random-oriented Cu and highly (111)-oriented Cu were 0.340 and 0.326, respectively.[24] The correlation coefficient of linear regression should be higher than 0.7 to confirm the accuracy of the stress values.[21]

## RESULTS AND DISCUSSION

The grain orientation in the two types of Cu films was observed by using a D8 DISCOVER in-house x-ray diffractometer. Figure 2 presents the x-ray diffraction results of random-oriented Cu and highly (111)-oriented Cu thin films under different bath temperatures. The random-oriented Cu thin film exhibited the highest intensity of (111) at a bath temperature of 35°C and a slight variation

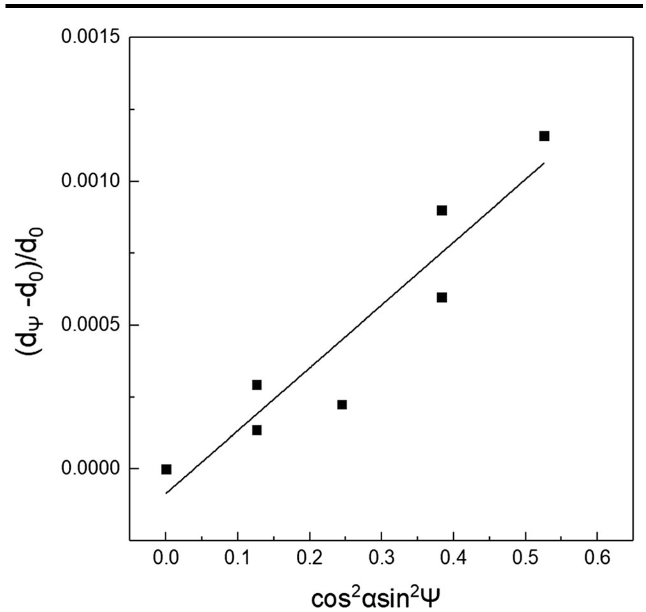


Fig. 1. Linear plot of $(d_\Psi - d_0)/d_0$ versus $\cos^2\alpha\sin^2\Psi$ from a highly (111)-oriented Cu thin film on Si substrate.

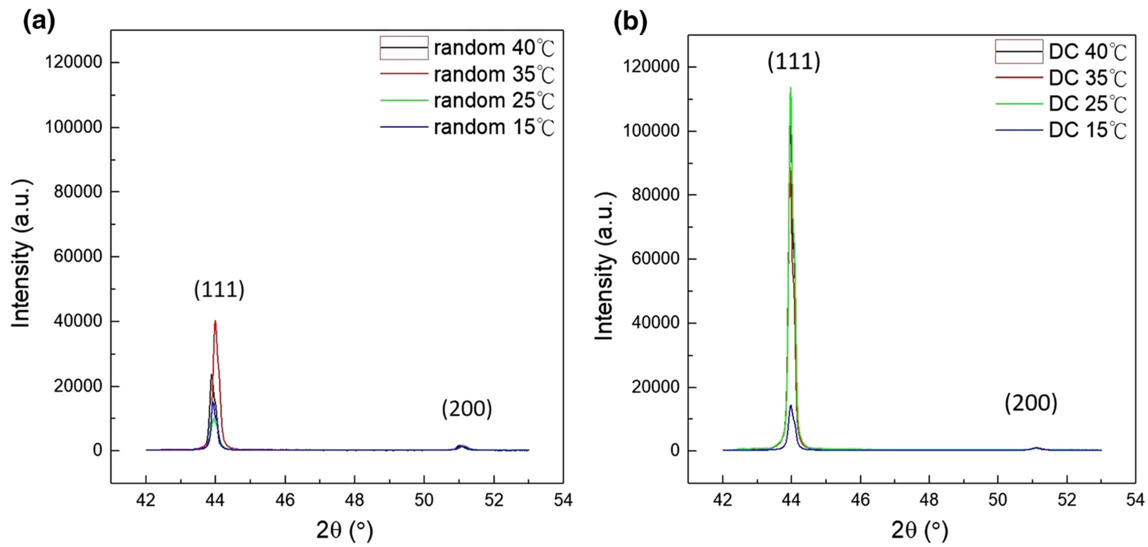


Fig. 2. X-ray diffraction patterns of (a) the random-oriented and (b) the highly (111)-oriented Cu thin films under different bath temperatures.

**Table I. The average grain size of highly (111)-oriented nt-Cu and random-oriented Cu thin films at different bath temperatures**

| Highly (111)-oriented nt-Cu | | Randomly oriented Cu | |
|---|---|---|---|
| Bath temperatures (°C) | Grain size ($\mu$m) | Bath temperatures (°C) | Grain size ($\mu$m) |
| 15 | 0.69 | 15 | 0.64 |
| 25 | 0.87 | 25 | 0.57 |
| 35 | 0.89 | 35 | 0.84 |
| 40 | 1.08 | 40 | 0.97 |

under different bath temperatures. The reason random-oriented Cu film had the highest (111) intensity at a bath temperature of 35°C is not clear. However, the highly (111)-oriented Cu thin films revealed a remarkable discrepancy of (111) as a function of bath temperature and reached the highest intensity at a bath temperature of 25°C. According to Figs. 4 and 6, the microstructure of nt-Cu films at a bath temperature of 25°C has high (111) orientation and a large number of columnar grains. This might explain why the results of the highest (111) intensity appeared at a bath temperature of 25°C.

The (111) grain orientation ratio in the highly (111)-oriented Cu intensity was one order of magnitude larger than that in the random-oriented Cu thin film.

The grain size is observed to increase with the increase of bath temperature. We apply OIM software and calculate the thin film grain size at different bath temperatures as shown in Table I. The grain size of random–oriented Cu thin film is 0.64 $\mu$m at 15°C and 0.97 $\mu$m at 40°C. The grain size of highly (111)-oriented Cu thin film is 0.69 $\mu$m at 15°C and 1.08 $\mu$m at 40°C. Figure 3 shows the EBSD images of the random-oriented Cu films under different bath temperatures. The Cu films with highly (111)-oriented grain orientation is observed for bath temperatures 25–40°C, while the Cu film prepared at bath temperature 15°C did not display (111) texture. Figure 4 depicts the (111) texture development upon tuning electrolyte temperatures for the highly (111)-oriented Cu films. We've discovered that highly (111)-oriented Cu films could not be fabricated at all at a low bath temperature of 15°C.

We employed a focused-ion beam to examine the microstructural evolution under different bath temperatures of the two types of Cu films. The cross-sectional images of the random-oriented Cu and the highly (111)-oriented Cu thin films under different bath temperatures are shown in Figs. 5 and 6. The microstructure was randomly oriented under all bath temperatures with the thicknesses controlled at 2.8 $\pm$ 0.2 $\mu$m as presented in Fig. 5. The (111)-oriented nanotwinned structure could be seen in the columnar grains of samples fabricated at bath temperatures between 25°C and 40°C with a thickness of 2.7 $\pm$ 0.2 $\mu$m in Fig. 6.

The residual stress measurement was determined by the $\cos^2\alpha\sin^2\Psi$ calculation with $\Phi$ angle scan.[21,22] The average stress of the two types of Cu films

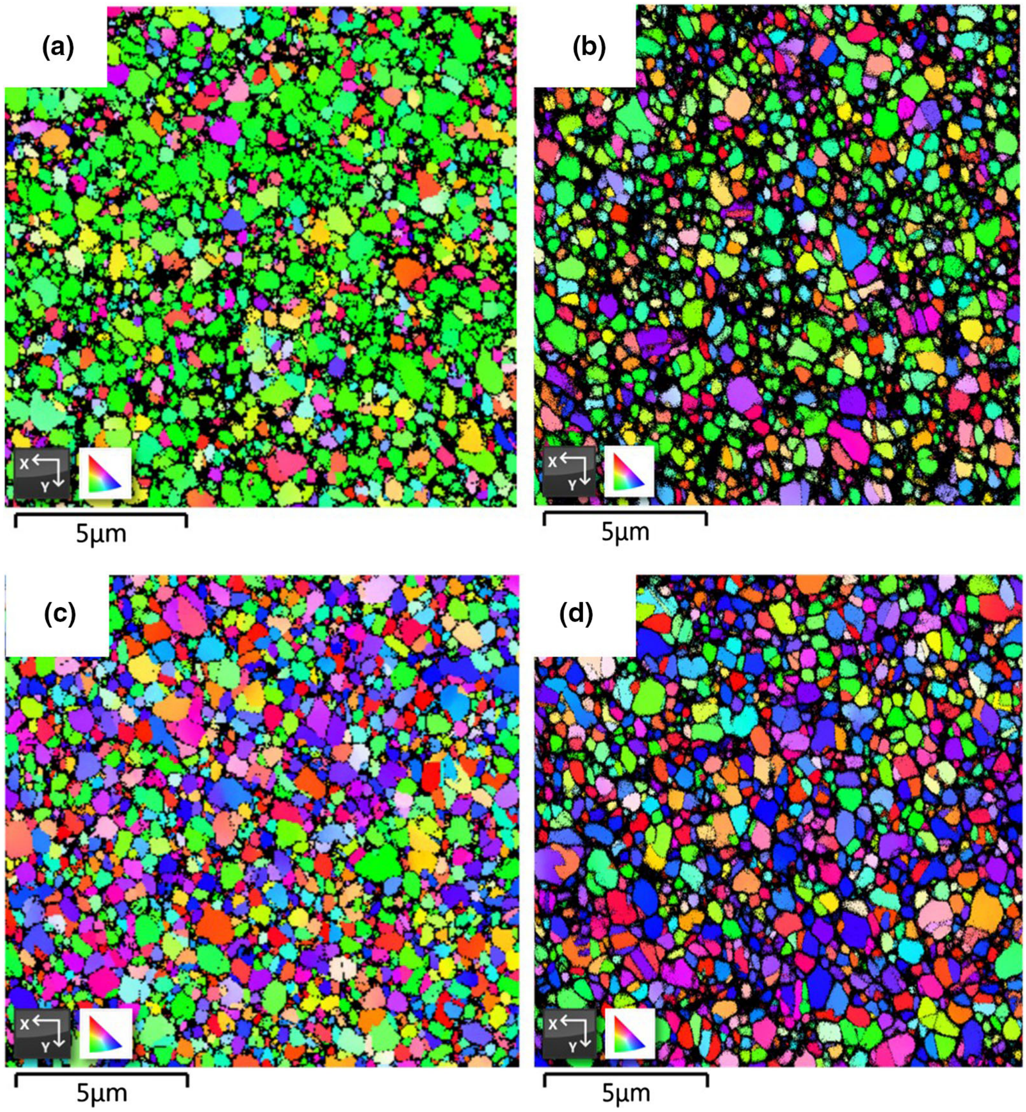


Fig. 3. EBSD images of the random-oriented Cu thin films at bath temperatures (a) 15°C, (b) 25°C, (c) 35°C, and (d) 40°C.

under different bath temperatures is shown in Fig. 7. The stress of the random-oriented Cu decreased with increasing bath temperature. The average stress has the smallest value of 33 MPa at the bath temperature of 40°C. The (111)-oriented nt-Cu has the smallest value of 95 MPa at a bath temperature of 35°C. Increasing the bath temperature from 15°C to 35°C decreased the average stress by 60%.

According to Chason et al's research,[25,26] the growth of thin film stress may be caused the parameter $D/RL$ where $D$ is the effective diffusivity, $R$ is the growth rate and $L$ is the grain size. If low temperature or high growth rate causes low $D/RL$ values, the calculated stress is tensile which means the atoms will have little time to diffuse into the triple junction and relieve the tensile stress created when grain boundary forms. If high temperature or low growth rate causes high $D/RL$ values, the calculated stress is less tensile or compressive so that there is enough time for atoms to diffuse into the triple junction and relieve the tensile stress. The theory calculation matches our experimental results and explains the evolution of stress.

Thin films with smaller grains have higher tensile stress[25] due to the dependence of the stress parameter on $L^{-1/2}$ so that smaller grains result in more grain boundaries and create tensile stress. However, at a low growth rate the stress is predicted to be more compressive because atoms have enough time to insert into triple junction and relieve the tensile stress. The growth rate must be lower than 0.05 nm/s for the situation to occur, but the lowest growth rate might be 4 nm/s in this research which is up to 100 times larger than that case.

The nanotwinned structure might be the reason that caused highly (111)-oriented Cu thin films to have large residual stress. The nanotwinned structure is a defect, which causes high stress. From Fig. 7a and b we see that the residual stress of

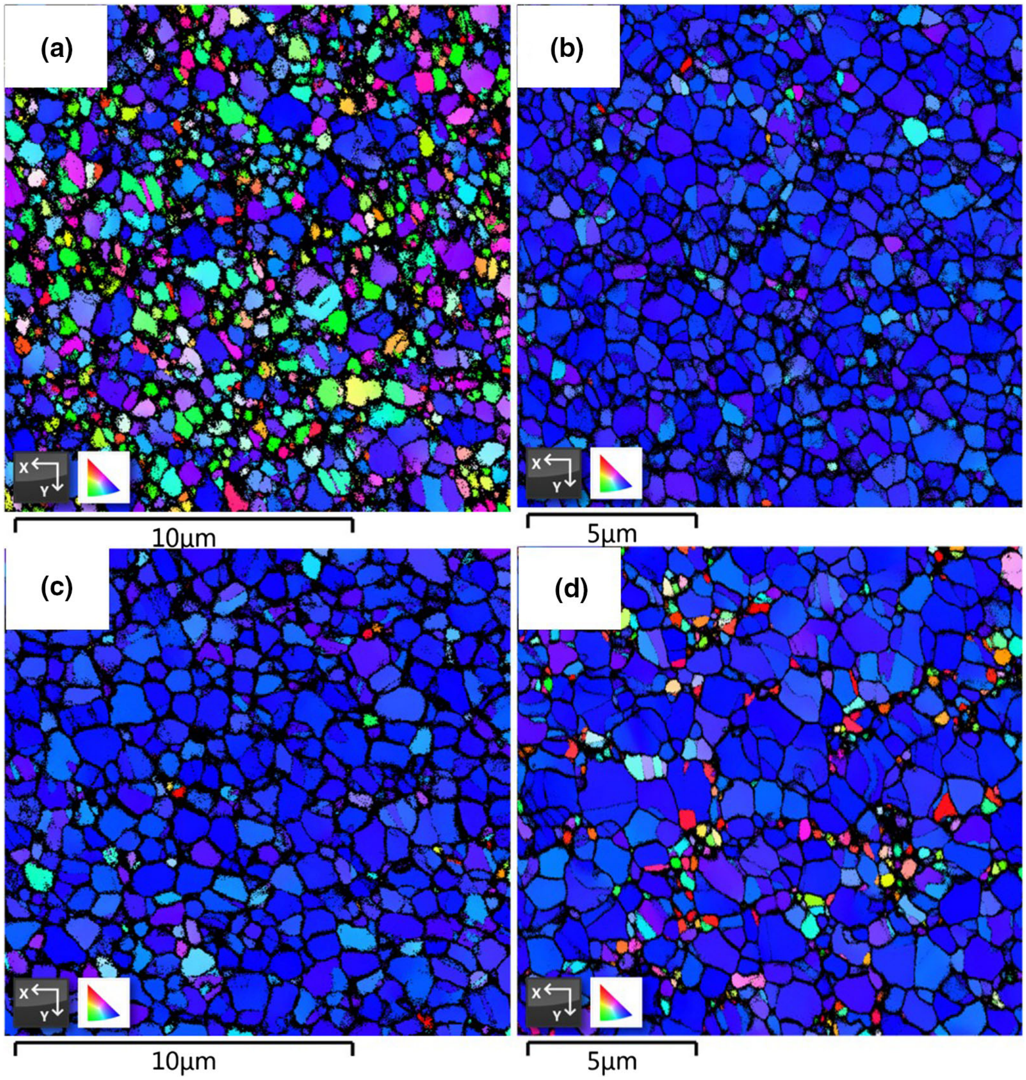


Fig. 4. EBSD images of the highly (111)-oriented Cu thin films at bath temperatures (a) 15°C, (b) 25°C, (c) 35°C, and (d) 40°C.

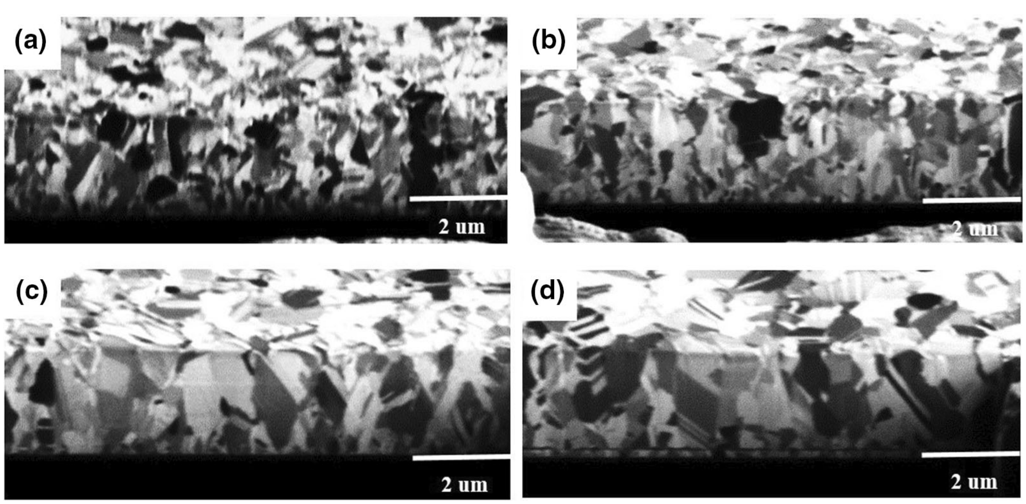


Fig. 5. The cross-sectional FIB images of the random-oriented Cu thin films at bath temperatures (a) 15°C, (b) 25°C, (c) 35°C, and (d) 40°C.

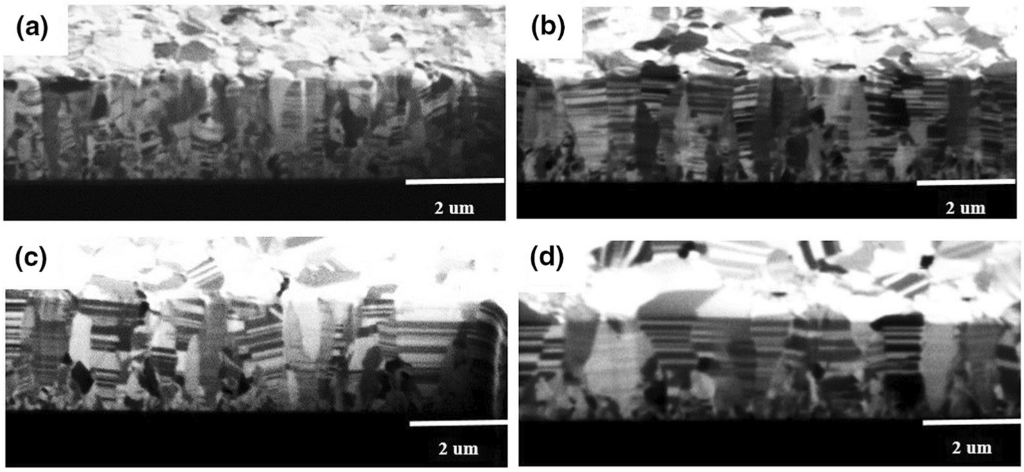


Fig. 6. The cross-sectional FIB images of the highly (111)-oriented Cu thin films at bath temperatures (a) 15°C, (b) 25°C, (c) 35°C, and (d) 40°C.

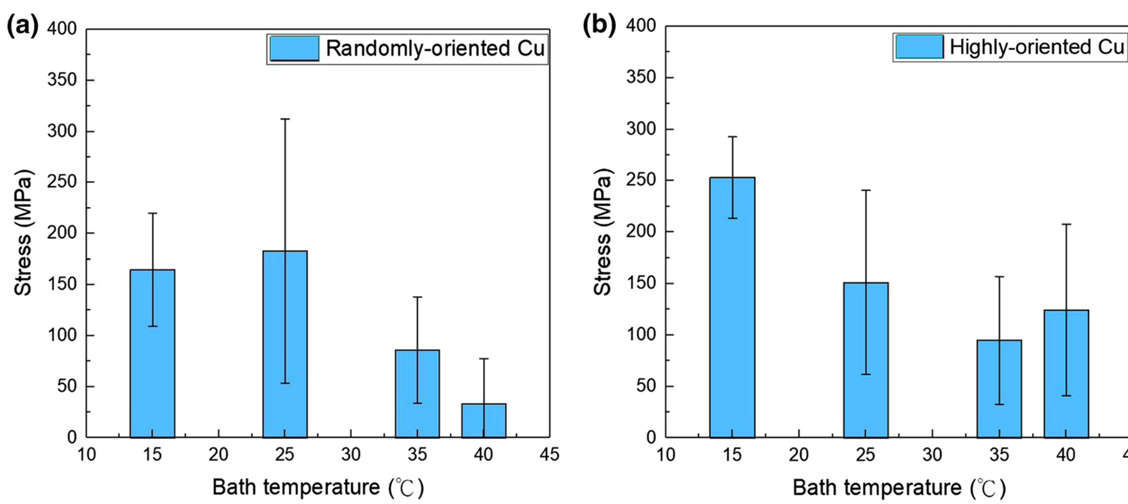


Fig. 7. The average stress of (a) the random-oriented and (b) the highly (111)-oriented Cu thin films under different bath temperatures.

highly (111)-oriented Cu thin films were all larger than random-oriented Cu thin films, which proves this point. From the results, it is observed that most data show a large deviation in our residual stress values. According to Ma et al.'s research,[22] Cu thin films with textured structures might not be uniform in the azimuthal direction, which leads to fluctuation of the residual stresses in azimuthal angles.

The findings indicate that nt-Cu films fabricated by electroplating at an optimal bath temperature of 35–40°C are able to reduce the residual stress of thin films. Besides tuning the stress, the nanotwinned structures can also enhance the mechanical strength in thin films, which have superior reliability to randomly oriented Cu thin films. We can fabricate nt-Cu thin films with the residual stress lower than 100 MPa. The residual stress is smaller than results of other articles,[27–30] since the Cu thin films in our research have good equality and performance.

Low bath temperature has a negative effect on residual stress in the nanotwinned structure. It is suggested that controlling the optimal bath temperature over 25°C is critical to reach high (111)-preferred orientation while also decreasing the residual stress.

Although the residual stress of highly (111)-oriented nt-Cu films were overall larger than random-oriented Cu films, we show that it is still possible to change the residual stress by different electroplating bath temperatures. While nanotwinned copper has notable advantages such as high thermal stability and high electromigration resistance,[14,15] by tuning the electrolyte bath temperatures we could further reduce the residual stress of highly (111)-oriented nt-Cu films.

## CONCLUSION

We can decrease the residual stress of copper thin films by increasing electroplating temperatures. At higher bath temperatures of 35°C, the highly (111)-oriented nt-Cu thin film has the lowest residual stress of 95 MPa. Meanwhile, the randomly oriented Cu thin film has the lowest residual stress of 33 MPa at bath temperatures of 40°C. The microstructure, grain orientation, grain size, and residual stress of Cu thin films were affected by different bath temperatures in the electroplating process. The grain size increases with increasing bath temperatures.

In this article we successfully tuned and measured the residual stress of Cu thin films. However, there is still much effort to make highly (111)-oriented Cu thin films suitable for future application, such as understanding their thermal behavior and thermal stress in further research. The residual stress of the as-deposited Cu thin films can help to better understand the film quality and life prediction in future reliability researches.

## ACKNOWLEDGMENTS

This work was financially supported by the "Center for the Semiconductor Technology Research" from the Featured Areas Research Center Program within the framework of the Higher Education Sprout Project by the Ministry of Education (MOE) in Taiwan. The work was also supported in part by the Ministry of Science and Technology, Taiwan, under Grant MOST-108-3017-F-009-003.

## REFERENCES

1. R.R. Schaller, *IEEE Spectr.* 34, 52 (1997).
2. V.S. Rao, C.T. Chong, D. Ho, D.M. Zhi, C.S. Choong, S.L. Ps et al., Development of high density fan out wafer level package (HD FOWLP) with multi-layer fine pitch RDL for mobile applications, in *2016 IEEE 66th Electronic Components and Technology Conference (ECTC)* (2016), pp. 1522–1529. IEEE.
3. J.H. Lau, 3D IC heterogeneous integration by FOWLP.*Fan-Out Wafer-Level Packaging*, ed. J.H. Lau (Singapore: Springer, 2018), pp. 269–303.
4. J.H. Lau, M. Li, D. Tian, N. Fan, E. Kuah, W. Kai, M. Li, J. Hao, Y.M. Cheung, Z. Li, and K.H. Tan, *IEEE Trans. Compon. Packag. Manuf. Technol.* 7, 1729 (2017).
5. G. Schlottig, A. Xiao, H. Pape, B. Wunderle, and L.J. Ernst, Interfacial strength of silicon-to-molding compound changes with thermal residual stress, in *2010 11th International Thermal, Mechanical & Multi-Physics Simulation, and Experiments in Microelectronics and Microsystems (EuroSimE)* (2010), pp. 1–5. IEEE.
6. J. Xi, D. Yang, L. Bai, X. Zhai, F. Xiao, H. Guo et al., Reliability of RDL structured wafer level packages, in *2013 14th International Conference on Electronic Packaging Technology* (2013), pp. 1029–1032. IEEE.
7. L. Lu, Y. Shen, X. Chen, L. Qian, and K. Lu, *Science* 304, 422 (2004).
8. D. Xu, V. Sriram, V. Ozolins, J.M. Yang, K.N. Tu, G.R. Stafford, C. Beauchamp, I. Zienert, H. Geisler, P. Hofmann, and E. Zschech, *Microelectron. Eng.* 85, 2155 (2008).
9. L. Lu, X. Chen, X. Huang, and K. Lu, *Science* 323, 607 (2009).
10. E. Ma, Y.M. Wang, Q.H. Lu, M.L. Sui, L. Lu, and K. Lu, *Appl. Phys. Lett.* 85, 4932 (2004).
11. R. Rosenberg, D.C. Edelstein, C.K. Hu, and K.P. Rodbell, *Annu. Rev. Mater. Sci.* 30, 229 (2000).
12. K.C. Chen, W.W. Wu, C.N. Liao, L.J. Chen, and K.N. Tu, *Science* 321, 1066 (2008).
13. K.C. Chen, W.W. Wu, C.N. Liao, L.J. Chen, and K.N. Tu, *J. Appl. Phys.* 108, 066103 (2010).
14. I.H. Tseng, Y.J. Li, B. Lin, C.C. Chang, and C. Chen, High electromigration lifetimes of nanotwinned Cu redistribution lines, in *2019 IEEE 69th Electronic Components and Technology Conference (ECTC)* (2019), pp. 1328–1332. IEEE.
15. Y.S. Huang, C.M. Liu, W.L. Chiu, and C. Chen, *Scripta Mater.* 89, 5 (2014).
16. C.H. Tseng, K.N. Tu, and C. Chen, *Sci. Rep.* 8, 1 (2018).
17. Yen-Chieh Chen and Chih Chen, *Study of Electrodeposition of Nanotwinned Cu Films at Different Bath Temperatures* (Hsinchu: Department of Materials Science and Engineering, National Chiao Tung University, 2017), p. 78.
18. A.F. Burnett and J.M. Cech, *J. Vac. Sci. Technol. A Vac. Surf. Films* 11, 2970 (1993).
19. M.N. James, *Eng. Fail. Anal.* 18, 1909 (2011).
20. C.M. Liu, H.W. Lin, C.L. Lu, and C. Chen, *Sci. Rep.* 4, 6123 (2014).
21. A.N. Wang, C.P. Chuang, G.P. Yu, and J.H. Huang, *Surf. Coat. Technol.* 262, 40 (2015).
22. C.H. Ma, J.H. Huang, and H. Chen, *Thin Solid Films* 418, 73 (2002).
23. Y. Zhou, C.S. Yang, J.A. Chen, G.F. Ding, W. Ding, L. Wang, M.J. Wang, Y.M. Zhang, and T.H. Zhang, *Thin Solid Films* 460, 175 (2004).
24. W. Köster and H. Franz, *Metall. Rev.* 6, 1 (1961).
25. E. Chason, J.W. Shin, S.J. Hearne, and L.B. Freund, *J. Appl. Phys.* 111, 083520 (2012).
26. E. Chason, B.W. Sheldon, L.B. Freund, J.A. Floro, and S.J. Hearne, *Phys. Rev. Lett.* 88, 156103 (2002).
27. R. Treml, D. Kozic, J. Zechner, X. Maeder, B. Sartory, H.P. Gänser, R. Schöngrundner, J. Michler, R. Brunner, and D. Kiener, *Acta Mater.* 103, 616 (2016).
28. R.M. Keller, S.P. Baker, and E. Arzt, *J. Mater. Res.* 13, 1307 (1998).
29. T. Hanabusa, K. Kusaka, and O. Sakata, *Thin Solid Films* 459, 245 (2004).
30. R.P. Vinci, E.M. Zielinski, and J.C. Bravman, *Thin Solid Films* 262, 142 (1995).